Financial price dynamics and pedestrian counterflows: A comparison of statistical stylized facts

Daniel R. Parisi,[1,2,*] Didier Sornette,[3,†] and Dirk Helbing[4,‡]

[1]*Instituto Tecnológico de Buenos Aires, 25 de Mayo 444, (1002) C. A. de Buenos Aires, Argentina*

[2]*Comisión Nacional de Investigaciones Científicas y Técnicas (CONICET), Argentina*

[3]*Department of Management, Technology and Economics, ETH Zürich, Scheuchzerstrasse 7, CH-8092 Zürich, Switzerland*

[4]*Chair of Sociology, in particular of Modeling and Simulation, ETH Zürich, Clausiusstrasse 50, CH-8092 Zürich, Switzerland*

(Received 14 May 2012; published 10 January 2013)

We propose and document the evidence for an analogy between the dynamics of granular counterflows in the presence of bottlenecks or restrictions and financial price formation processes. Using extensive simulations, we find that the counterflows of simulated pedestrians through a door display eight stylized facts observed in financial markets when the density around the door is compared with the logarithm of the price. Finding so many stylized facts is very rare indeed among all agent-based models of financial markets. The stylized properties are present when the agents in the pedestrian model are assumed to display a zero-intelligent behavior. If agents are given decision-making capacity and adapt to partially follow the majority, periods of herding behavior may additionally occur. This generates the very slow decay of the autocorrelation of absolute return due to an intermittent dynamics. Our findings suggest that the stylized facts in the fluctuations of the financial prices result from a competition of two groups with opposite interests in the presence of a constraint funneling the flow of transactions to a narrow band of prices with limited liquidity.

DOI: 10.1103/PhysRevE.87.012804 PACS number(s): 89.65.Gh, 45.70.Vn, 05.40.−a, 89.90.+n

I. INTRODUCTION

Analogies between complex flows and financial markets are not new. In 1996, Ghashghaie *et al.* have shown that the distribution of velocity increments of fully developed turbulence and that of exchange rate fluctuations exhibit striking similarities [1]. This led these authors to suggest a common connection via the existence of cascades in both systems, a Kolmogorov energy cascade in turbulence [2], and an information cascade in finance. However, Arneodo *et al.* [3] remarked that the two problems differ on the fundamental property of correlations and higher-order statistics. Indeed, spatial correlations in turbulence lead to the famous $-\frac{5}{3}$ power law for the spectrum of the velocity fluctuations [2], while no temporal correlations of this sort are visible in the power spectrum of financial time series. If such correlations existed in finance, it would be easy to use them to earn money, while the core of the problem in turbulence is the existence of very strong correlations. The analogy between turbulence and finance just based on a one-point statistics turned out to be a dead end. Let us also mention the formalism of Vamoş *et al.* [4] that counts the flux of price changes in a universe of assets, which is similar to a hydrodynamic conservation equation.

Perhaps less fancy than hydrodynamic turbulence but more appropriate, Bouchaud *et al.* [5] have suggested an analogy with molasses, the rock conglomerates that form as a result of geological sedimentary processes. They proposed a model of financial fluctuations based on the competition between liquidity providers and liquidity takers, in which the existence of an excess flow of limit orders opposing the market order flow together with a systematic anticorrelation of the bid-ask motion between trades lead to create a "liquidity molasse" which dampens market volatility. Another physics-inspired approach was to model the price formation process via the order book dynamics as diffusing annihilating particles in one dimension [6,7].

In the present work, we identify an additional complex flow that amazingly displays most of the statistical properties of financial time series. This flow consists of a simulated system representing a pedestrian counterflow throughout a door (i.e., a bottleneck). The suggestion of a similarity between pedestrian counterflows throughout constrictions and financial markets was first proposed by Helbing [8,9]. The first supportive evidence of this idea was reported by Parisi [10], considering the mean velocity near the door as the observable of the pedestrian system. The fact that pedestrian flows can exhibit rich behaviors similar those found in other complex systems, such as a kind of turbulent behavior, has also been documented [11,12].

We find that the dynamics of the density fluctuations at the location of the bottleneck reproduces eight stylized facts already documented for financial price fluctuations [13–18]. This degree of quantitative likeness is remarkable and has very rarely been achieved by agent-based models or econometric models designed to represent financial markets. The reproduction of the eight stylized facts is especially noteworthy, considering that the pedestrian system simulated here was not created to reproduce the financial market characteristics.

In our study, we consider the cases of zero-intelligent pedestrians or particles that follow mechanical rules and the extension where pedestrians can change their strategy by imitating the majority. The later ingredient turns out to be necessary to generate the equivalent of bubbles and crashes, while the other stylized facts remain the same.

The paper is organized as follows. In Sec. II, we describe the simulated pedestrian system and the price time series used for comparison. Section III presents the analysis of the eight statistical properties mentioned above, obtained from

*dparisi@itba.edu.ar
†dsornette@ethz.ch
‡dhelbing@ethz.ch

simulations of the constrained pedestrian system and from empirical financial data. In Sec. IV, the implications of our findings are discussed. Section V presents the conclusions.

II. FINANCIAL AND PEDESTRIAN TIME SERIES

A. Financial data

Data from foreign exchange rates and stock indexes were analyzed in order to compare their stylized properties with those produced by a pedestrian simulation model. Specifically, we evaluated the following data: EURUSD-1min, EURUSD-10min, EURUSD-1hour, CHFUSD-1hour, Nasdaq100-1hour, DJI-1day, NYSE100-10min, NYSE100-1hour, and NYSE100-1day. The financial time series contained between 10 000 and 30 000 data points and were taken from public Internet sources [19,20].

B. Pedestrian model and setup

1. Description of the model

Our pedestrian simulations were based on the social force model [21]. In this model, pedestrians are treated like circular disks with different radii representing the space occupied by them. The dynamics of each pedestrian (i) is governed by three forces: the "driving force" ($\mathbf{F}_{\mathrm{Di}}$), the "contact force" ($\mathbf{F}_{\mathrm{Ci}}$), and the "social force" ($\mathbf{F}_{\mathrm{Si}}$). The driving force is responsible for the self-propulsion of each simulated pedestrian ("agent"), and it provides a constant input of energy into the system. The contact force is a dissipative and repulsive interaction force between particles that appears only when at least two particles overlap. The specifications of these two forces and the parameter values were chosen as in Ref. [21]. However, in the present case, the social force is assumed to be repulsive locally and attractive at a larger distance, as defined by Eqs. (1) and (2),

$$\mathbf{F}_{\mathrm{Si}} = \sum_{j=1,\, j\neq i}^{N_p} A(d_{ij}) \exp\left(\frac{-d_{ij}}{B}\right)\mathbf{e}_{ij}^{n}. \qquad (1)$$

Here, N_p is the total number of pedestrians in the system, $\mathbf{e}_{ij}^{n}$ is the unit vector pointing from pedestrian j to i (the "normal" direction), d_{ij} is the edge-to-edge distance between both pedestrians (defined as the distance between their centers minus the sum of their radii, as in Ref. [21]), $B = 0.08$ m is a constant determining the range of the social interaction, and A is

$$A(d_{ij}) = \begin{cases} +2000\ \mathrm{N} & \text{if} \quad d_{ij} < 0.15\ \mathrm{m}\ \text{(repulsive)} \\ -2000\ \mathrm{N} & \text{if} \quad d_{ij} > 0.15\ \mathrm{m}\ \text{(attractive)} \end{cases}, \qquad (2)$$

where N stands for the unit of force in newtons. For the interaction of a pedestrian i with a wall (w), the value of A is assumed to be greater than zero for all d_{iw} (i.e., the wall has only a repulsive effect).

The pedestrians parameters, namely mass (m), diameter ($2r$), and desired velocity (v_d), were uniformly distributed within the following ranges: $m \in$ [70 kg, 90 kg], $2r \in$ [0.44 m, 0.56 m], and $v_d \in$ [1.05 m/s, 1.35 m/s],

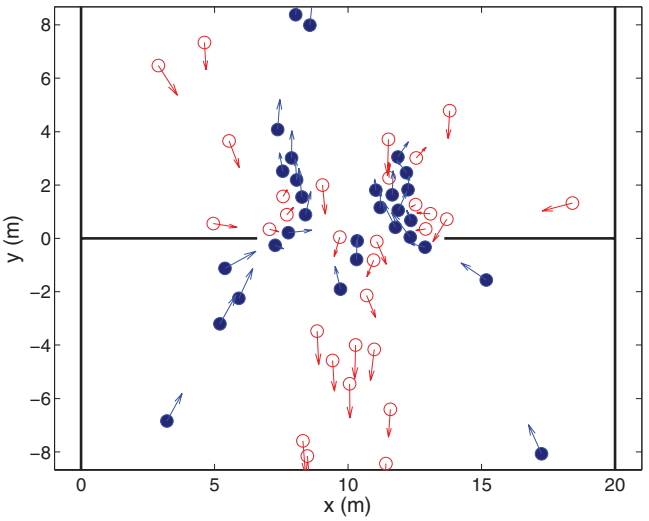

FIG. 1. (Color online) Setup of our simulation of pedestrian counterflows. The two kinds of particle filling indicate the state of the pedestrians. The arrows display their current velocities.

2. The simulated pedestrian system

Our simulation of pedestrian counterflows is based on two open corridors of 20-m width, connected by a door of width L, as shown in Fig. 1. Initially, there are $N_p/2$ agents on each side of the door. These agents attempt to reach, first, the door and then the end of the corridor on the other side. In order to achieve this goal, the pedestrians must cross the door in opposite directions, and, thus, a counterflow is created.

More specifically, the driving force is dynamically adjusted in order to aim agents at the nearest point laying on a segment of length $(L - 2l)$ parallel to the line of the door, whose center coincides with the center of the door. After reaching this line, pedestrians move toward a second target located 10 m away from the door ($x = 10$; $y = \pm 10$, in the coordinate system of Fig. 1). Once a particle reaches a target placed 10 m away from the door, it is instantaneously reinserted at a random position in the corridor where it started (not more than 10 m from the door). In this way, a continuous counterflow is established with a fixed number of particles. This mechanism describes an automaton-like behavior of agents in the sense that they have a unique objective: to reach their assigned target, no matter where they are. We call this version of the counterflow system "automata pedestrians" or "automata agents."

3. Agents with decision-making capacity

There is rich literature in psychology, behavioral finance, and agent-based models which includes some herding in the behavior of agents and investors. Let us mention the work of Lillo *et al.* [22], which considers the mechanism of inventory variations and its correlation with the stock return. We mention it as it is the closest in spirit to the mechanics of decision making that we implement in our model.

In the pedestrian system described above, there are two groups of "automata agents" with opposite, but fixed, flow directions; let us call them a and b. Because the number of agents belonging to each class is fixed ($N_a = N_b$), the system is forced to be in a statistical equilibrium from a population point

of view. The model can be generalized by allowing agents to change their state via a decision mechanism. The system then is able to exhibit collective or herding behavior of the agents. For example, all agents could choose to be in the same state, i.e., to have the same desired walking direction. This situation is analogous to a financial crash, when all agents want to sell their assets. Thus, when considering pedestrians or agents with decision-making capacity, two different situations may occur: equilibrium ($N_a \sim N_b$) or herding ($N_a \gg N_b$ or $N_a \ll N_b$).

In our system, the decision mechanism works as follows. Each particle reaching the line of the door must choose between keeping and changing its state (from a to b or vice versa). In each cycle of reinsertion, this decision is made only once when a pedestrian enters a rectangular area A of size $L \times 1$ m, extending 50 cm to both sides of the door. For the deciding pedestrian i, the following fraction is calculated,

$$\xi_i = \frac{n_s}{(n_s + n_d)}, \tag{3}$$

where n_s is the number of agents in the same state as agent i and n_d is the number of agents in the other state (with an opposite desired walking direction). Note that $n_s + n_d$ is the total number of agents in the area A. Then, the decision is made by choosing a random number (χ) from a uniform distribution in the interval [0, 1] and comparing it with a sigmoid function,

$$F(\xi) = \frac{1}{1 + \exp\left[\frac{-(\xi - 0.5)}{T}\right]}. \tag{4}$$

If $F(\xi_i) < \chi$, then agent i changes its state. Because of the shape of this function, it is more probable to change state if the particles are in a minority. In other words, if pedestrian i is in the minority, it is more likely to join the state of the majority.

The parameter T is treated as a behavioral parameter. When this parameter is low, the agents tend to show herding behavior, which means that they have a greater tendency to imitate the behavior of neighbors. On the contrary, when T tends to infinity, the agents ignore the state of their neighbors. Therefore, we call T the "individualistic" parameter.

As T goes to 0, $F(\xi)$ approaches to the step function, which describes a deterministic rather than probabilistic decision behavior (agents in the minority side will change their state and agents in the majority side will never change their state). In this extreme case, the number of particles of one type will saturate and this state will not be reverted.

An equilibrium between both populations is achieved if T tends to ∞. Then $F_{(\xi)}$ become 0.5, which makes the decision totally random for each agent. No matter what the fraction of particles of one kind (ξ) is, the decision to change the state is made with probability 1/2. In this case, the number of particles of each type fluctuates around the equilibrium value $N_a \sim N_b \sim N_p/2$ (=50% of the population).

III. RESULTS

After having experimented with different observables, we find that the dynamics of the pedestrian density exhibits the closest correspondence with that of prices in financial systems. In the following, we will explore the analogy between (a) the financial time series introduced in Sec. II A and (b) the density of pedestrians around the door according to the models described in Sec. II B. We will study both agents without and with decision-making capacity (see Secs. II B2 and II B3). This will be done by analyzing the statistical properties of the return and related quantities defined in the next subsection.

A. Density versus logarithm of the price

Let Y be any general time series. Then, we defined the return as

$$R_Y = \frac{dY}{dt}. \tag{5}$$

For a discrete time series, the discretely sampled return is

$$R_Y^k = Y(t_i + k) - Y(t_i), \tag{6}$$

where t_i indicates the discrete time steps and k the number of time steps over which the return is computed. In the particular case of an asset price (S), we take $Y = \ln(S)$, where S is the asset price and $k = 1$. Then Eq. (6) becomes the well-known logarithmic return for financial time series $R = \{\ln[S(t_i + 1)] - \ln[S(t_i)]\}$.

Now, for a general time series Y, we define the absolute value of the return by

$$\left|R_Y^k\right| = |Y(t_i + k) - Y(t_i)| \tag{7}$$

and the standardized absolute return (inspired by the standardized return [23,24]) by

$$\left|\hat{R}_Y^k\right| = \frac{\left|R_Y^k\right|}{\left(\sum_{t_i=1}^{N_T-k} \left|R_Y^k\right|\right)/(N_T - k)}, \tag{8}$$

where N_T is the total number of data points in the time series Y. Therefore, the denominator is the arithmetic mean of the absolute return.

As stated above, for a price time series S, it is common to consider the logarithmic return by taking $Y = \ln(S)$. In the case of the pedestrian system, the time series to be analyzed is the density, i.e., $Y = \rho$. We calculate the density as the average density over three equidistant points on the door line by using the κ nearest-neighbor algorithm (κ-NN) with $\kappa = 8$. This algorithm consists in measuring the distance (d_κ) to the κ^{th} nearest neighbor from any point (x_0, y_0), and so the density in that point can be approximated as $\rho_{(x_0,y_0)} = \frac{(\kappa-1)}{\pi(d_k)^2}$.

All the stylized facts, for the time series from both systems, are observed for the return and related quantities defined above.

B. Automata agents

In this subsection, we study the stylized facts of the pedestrian system of automata agents as described in Sec. II B. These are compared with those emerging from financial markets. The parameters characterizing the pedestrian system are $L = 7$ m, $l = 0.2$ m, and $N_p = 60$ (30 pedestrians in state a and 30 in state b all the time). The total number $N_p = 60$ of particles used in our simulations should be compared with the number (approximately 600) that would correspond to a random close packing. Hence, the density of particles is comparable to a dense gas for which the effect of the constriction is essential for the properties described below to emerge.

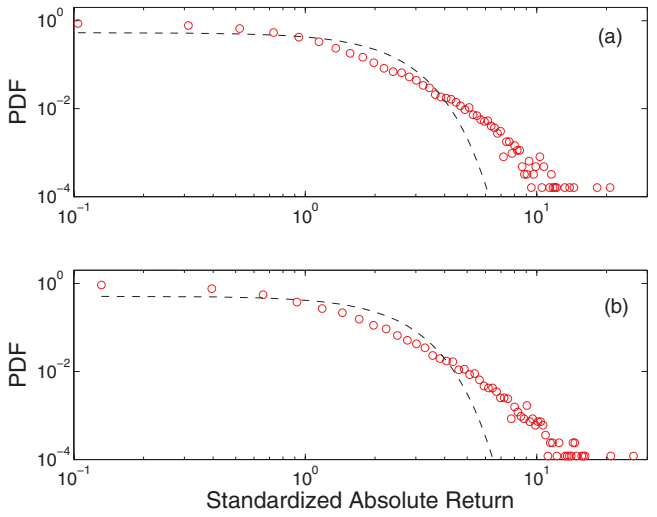

FIG. 2. (Color online) Probability density functions (PDF) of the standardized absolute returns of the time series ρ for simulated automata pedestrians (a) and of the time series $\ln(S)$ for the EURUSD-1hour currency exchange data (b). The dashed lines indicate the closest Gaussian distribution as a guide to the eye to reveal the fat tails of both PDF.

1. Heavy tails

An important characteristic of distribution functions of return of financial time series is that they exhibit fatter tails than a Gaussian distribution [25]. In order to make both time series comparable, we take the standardized absolute return. Figure 2 shows both distributions, where the dotted line indicates the closest Gaussian distribution as reference. It can be seen that both distributions exhibit fat tails and look very similar.

2. Aggregational Gaussianity

As seen in Eqs. (6)–(8), for discrete time series, the return can be calculated over different periods of time, parameterized by the number of time steps ($k = 1,2,\ldots$). It is known for financial data that, as the number of time steps k increases, the distribution of the return converges against a Gaussian distribution [14,26]. Figure 3 shows this tendency for $|\hat{R}^k_\rho|$ for the pedestrian system.

3. Autocorrelation of return and volatility

Asset returns show no linear autocorrelation, except for very small time scales. However, the volatility displays a positive autocorrelation. This indicates that big price fluctuations are often followed by big price fluctuations, a fact which is known as "volatility clustering" [14,27–29]. Taking the absolute return as a measure of the volatility, we compare the autocorrelation function of the return and the absolute return for the pedestrian time series (Fig. 4).

The plot reveals that the system of automata agents presents an autocorrelation of absolute returns that is greater than the autocorrelation of returns. Although this phenomenon is visible in the pedestrian system, the decay of the autocorrelation function of absolute returns is much slower in financial time series. This stylized property will become more similar in the

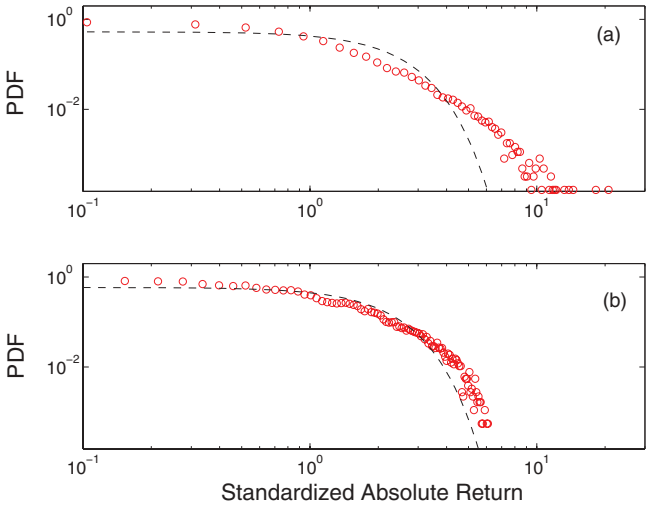

FIG. 3. (Color online) Probability density function of the standardized absolute return of ρ with $k = 1$ (a) and $k = 100$ (b). The dashed line indicates the closest Gaussian distribution.

two time series when decision-making capacity is added to agents (see Sec. III C2).

4. Scaling of the peaks of the distribution of returns

As in Sec. III B2, we calculate here the return [R^k_ρ and $R^k_{\ln(S)}$] for different time intervals k. For the pedestrian system and FX markets, the probability distribution of returns is symmetrical (zero skewness) and has a peak at zero return. It was shown in Ref. [30] that the S&P500 index exhibits a power-law scaling behavior when the probability of zero return [$P_{(R=0)}$] is plotted against the time interval k. In our case, we approximate the probability of return $R^k = 0$ by computing the kernel density estimator [31]. The values of k considered were $k = 1,6,11,\ldots,101$. Figure 5 displays a log-log plot of the probability [$P_{(R=0)}$] versus k. The figure shows that the scaling property exists also in the pedestrian system.

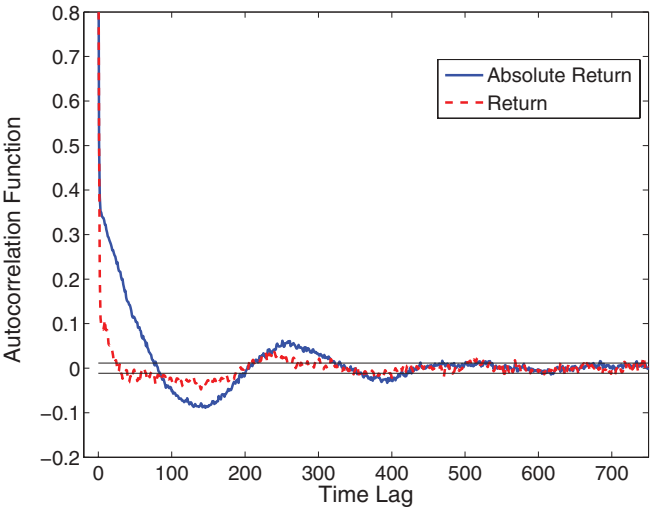

FIG. 4. (Color online) Autocorrelation functions of the return and absolute return of the density time series for automata pedestrian system.

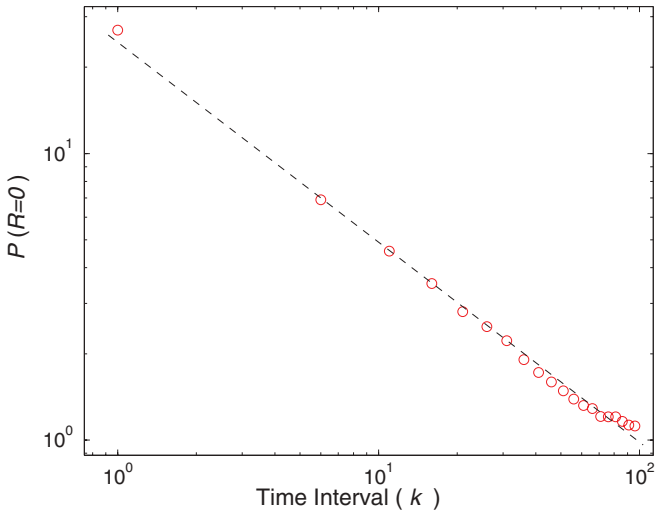

FIG. 5. (Color online) Maxima of the distributions of returns R^k_ρ versus the number k of time steps.

Furthermore, the value of the power-law exponent is $\alpha = -0.70$, very similar to the one observed for financial data: EURUSD-1min ($\alpha = -0.71$), EURUSD-10min ($\alpha = -0.77$), and CHFUSD-1hour ($\alpha = -0.67$). Moreover, Ref. [30] reports $\alpha = -0.71$ for S&P500.

5. Multifractality

Multifractality can be tested by examining the ratio $\langle |R^k|^q \rangle / \langle |R^k| \rangle^q$ for returns calculated with different time steps k. This ratio is constant for a simple fractal but not for a multifractal [28]. Figure 6 shows this plot for the pedestrian system considering $q = 1.5$, 2, 2.5, and 3.

If we take the slope of the higher curve ($q = 3$) as a measure of multifractality (-0.16), it is very similar to the ones obtained for financial time series (ranging from -0.13 to -0.18).

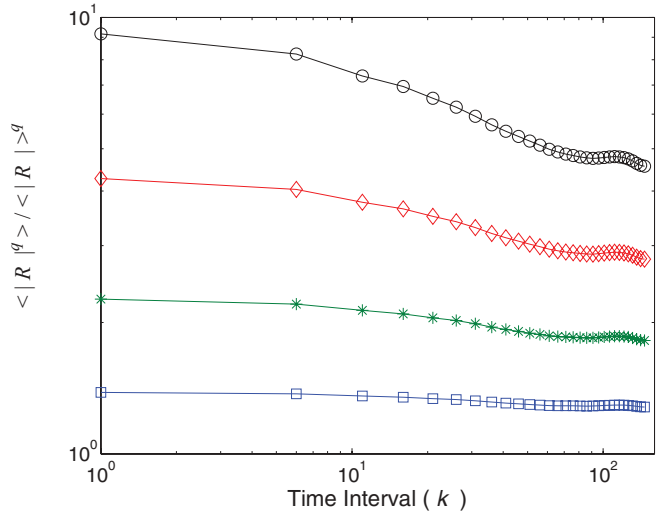

FIG. 6. (Color online) Ratio $\langle |R^k_{(\rho)}|^q \rangle / \langle |R^k_{(\rho)}| \rangle^q$ versus number k of steps over which the return is calculated for $q = 1.5$ (blue square), 2 (green star), 2.5 (red diamond), and 3 (black circle).

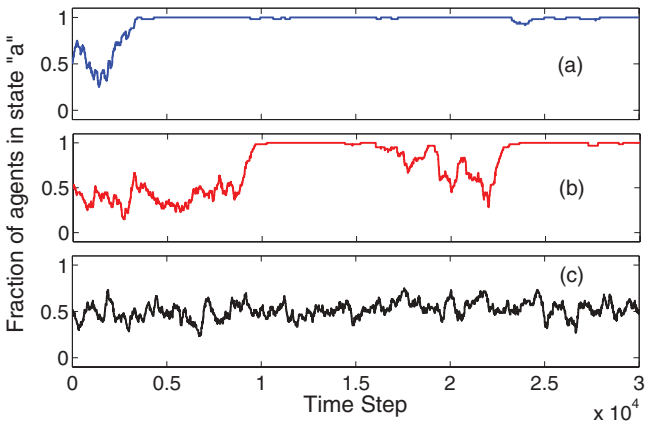

FIG. 7. (Color online) Comparison of the fraction $\frac{N_a}{N_p}$ for three realizations for different values of the individualistic parameter: (a) $T = 0.071$ (saturated regime), (b) $T = 0.078$ (transition regime), and (c) $T = 0.150$ (nonsaturated regime).

6. Hurst exponent

Self-similarity of the signal is an important feature and has been largely studied for financial systems [32–34]. In this subsection, we calculate the Hurst exponent (H) of the absolute return time series ($|R_Y|$). This study was also performed in Ref. [33] by analyzing four major stocks from the London Stock Exchange.

We calculate H using the detrended fluctuation analysis (DFA) [34,35]. The value of H obtained for the pedestrian system is $H = 0.88$, which is similar to the ones obtained for DJI-1day ($H = 0.86$) and NYSE100-1day ($H = 0.85$). Furthermore, the results reported in Ref. [33] are also similar, ranging from $H = 0.80$ to $H = 0.86$. The other financial time series analyzed in the present work display values of $H \geqslant 0.65$. In all cases, the results show that self-similarity is present, and the Hurst exponent lies in the region $0.5 < H < 1$, which corresponds to correlated noise, indicating long-term memory of the absolute return.

C. Pedestrians with decision-making capacity

In previous sections, we analyzed the statistical properties of the pedestrian system for automata agents; here we will study the properties when we provide simulated pedestrians with a decision-making capacity. As explained in Sec. II B3, this allows us to consider herding effects, so the system may develop a behavior similar to financial bubbles and crashes.

The parameters of the system for this behavior are the same as before, $L = 7$ m, $l = 0.2$, m and $N_p = 60$. At time $t = 0$, we assume again $N_a = N_b = N_p/2 = 30$, but as the system evolves, N_a and N_b will change.

1. Variations in the decision parameter

Similarly to the "herding indicator" defined in Ref. [22], we choose as a relevant observable the fraction of particles in a certain state, for example, let us take the state a. Figure 7 shows the evolution of the fraction N_a/N_p for three different values of T.

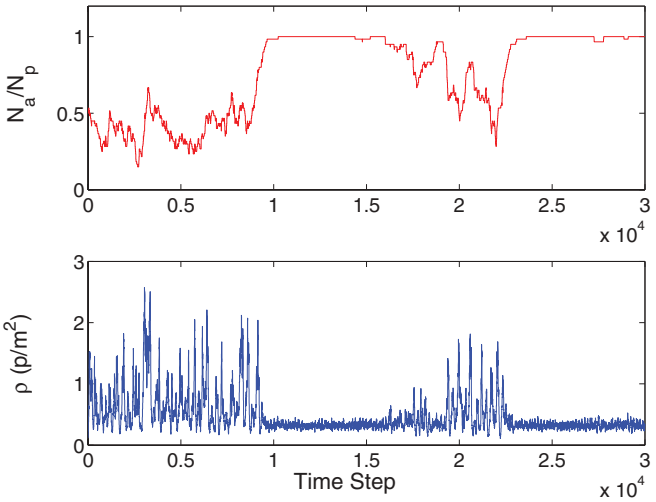

FIG. 8. (Color online) Fraction of the population $\frac{N_a}{N_p}$ for $T = 0.078$ (top) and related pedestrian density time series (bottom).

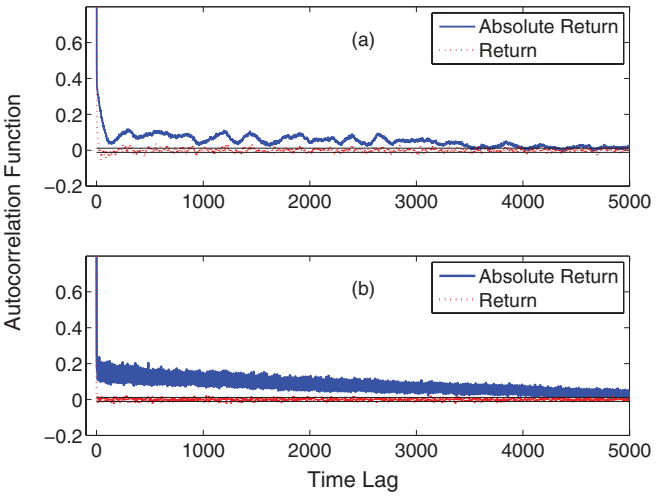

FIG. 9. (Color online) Autocorrelation functions of the return and absolute return for pedestrians with $T = 0.078$ (a) and for EURUSD-1hour financial data (b).

The system can be found in three different regimes.

(i) Saturated regime: For low values of the individualistic parameter ($T \lesssim 0.07$), the system saturates rapidly, indicating that all simulated pedestrians have the same state and, thus, a unidirectional flow is established.

(ii) Nonsaturated regime: For $T \gtrsim 0.09$, the system oscillates around $N_a/N_p \sim 1/2$. In this regime, the system behaves very similar to automata agents (Sec. III B).

(iii) Transition regime: For $0.07 \lesssim T \lesssim 0.09$, the behaviors of the saturated and nonsaturated regimes may be combined in the same realization (see middle panel of Fig. 7).

When the system remains saturated, all pedestrians end up acting in the same way. This situation might be analogous to stock market panic generating a financial crash. In fact, saturation periods are correlated with low values of the density time series ($0.2\,\mathrm{p/m^2} \lesssim \rho \lesssim 0.5\,\mathrm{p/m^2}$), as shown in Fig. 8. This feature further justifies the analogy between the pedestrian density (ρ) and the logarithm of the price ($\ln(S)$).

We observe that if only periods of unidirectional flow occur, all stylized facts disappear. Therefore, having two groups of agents with opposite goals (counterflow) is of fundamental importance for the emergence of the stylized facts studied in this paper.

2. *Autocorrelation of return and volatility*

Consider the nonsaturated regime ($T \gtrsim 0.09$) in which the number of pedestrians belonging to each group (N_a or N_b) fluctuates around the equilibrium value $N_p/2$. In this situation, the autocorrelations are very similar to the one observed in Fig. 4 for automata agents where the number of pedestrians in each state is fixed ($N_a = N_b = N_p/2$). However, for values of T in the transition zone ($0.07 \lesssim T \lesssim 0.09$), the time period above which the autocorrelation of the absolute return becomes negligible is much larger, in accordance with financial time series. In Fig. 9, it can be seen that both systems have a similar autocorrelation function of returns and absolute returns.

This result for the pedestrian system holds, in general, for T in the transition regime. The length of the decay of the autocorrelation depends on the coexistence of periods of saturation and nonsaturation of the population in the same realization, which is more likely to occur near $T \sim 0.08$.

It is important to stress that, in the saturated regime (corresponding to the unidirectional flow), all stylized facts (and in particular the autocorrelation of absolute return) disappear. While in the nonsaturated regime with permanent counterflow ($T \gtrsim 0.09$), the autocorrelation of absolute return is weak (see Fig. 4), independently of whether decision-making capacity is considered. Thus, it is interesting to discover that the significant autocorrelation of absolute returns can be understood by the combination of the two different regimes (the saturated and nonsaturated ones). In other words, this stylized fact appears when the pedestrian system is in the transition area between the saturated "herding" regime and the nonsaturated "equilibrium" regime. Such behavior is also found in other systems, such as generalized Ising models for which the excess volatility that is typical of real financial markets is obtained in the transition region of the underlying Ising critical point [36].

IV. DISCUSSION

We have shown in previous sections that a simple multiagent model simulating the counterflow of pedestrians displays eight stylized facts that are characteristic of a real complex social system, namely the financial market. Because these statistical properties taken together are very restrictive, one is led to hypothesize that the pedestrian system must have something in common with the financial one. In the following, we outline the key ingredients present in both systems.

First, we present arguments supporting the hypothesis that density and price are related. For conservative flows, in particular pedestrian flows, the continuity equation can be written as

$$\frac{\partial \rho}{\partial t} = -\vec{\nabla} \cdot \boldsymbol{J}, \tag{9}$$

where ρ is the density (measured in number of pedestrians/m^2) and $\boldsymbol{J}(=\rho \boldsymbol{v})$ is the pedestrian flow (number of pedestrians

crossing a unit length per unit time). The negative divergence of $\boldsymbol{J}$ [right-hand side of Eq. (9)] reflects the difference between particles entering and exiting a given area around the door.

We may interpret $-\vec{\nabla}\cdot\boldsymbol{J}$ in analogy with the difference between buy and sell orders (i.e., orders that want to enter into the position and orders which tend to exit the position). This difference will change the price, in a financial context, in a way similar to how $-\vec{\nabla}\cdot\boldsymbol{J}$ will change the density in the pedestrian system, i.e., via a linear impact function as argued theoretically as a result of the optimal order execution strategy [37] and the absence of arbitrage [38]. Here, we do not enter the debate on the underlying mechanism of possible nonlinear impact functions [39,40]. Because, for a price time series (S), the logarithmic return is defined as $R = \frac{d(\ln(S))}{dt}$, it is therefore reasonable to compare ρ with $\ln(S)$.

Second, consider systems endowed with the following attributes:

(a) Competition in the form of opposite tendencies, such as counterflows of particles moving in opposite directions, buyer-seller opposite drives to acquire versus drop an asset, or liquidity providers and takers with opposite needs with respect cash and access to markets;

(b) Bottleneck, restriction, or constriction that provide a convergent constraint in the free flow in the system; in granular flows, this is in the form of a funnel or an opening separating two different spatial domains; in finance, this is associated with the fact that actual transactions occur in the limit of small or vanishing liquidity [41]. In other words, whatever their volume, all orders have to be funneled to a small price window in order to be executed.

We conjecture that these systems operate in a "prejammed" state with large intermittent fluctuations that exhibit the following set of stylized facts:

(1) fat tail distribution of fluctuation amplitudes of some order parameter such as density variations or log-price variations;

(2) tendency for the above distributions to converge slowly to the Gaussian law at large space or time scales over which the order parameter fluctuations are measures;

(3) weak and fast decaying auto-correlation of the signed fluctuations of the order parameter;

(4) long-range auto-correlation of the amplitude (or "volatility") of the order parameter fluctuations;

(5) Hurst exponent and persistence in the dynamics of the volatility;

(6) scaling of the peaks of the distribution of the order parameter fluctuations;

(7) multifractality; and

(8) existence of transient coherent regimes (bubbles, solitary waves, coherent structures) bursting in crashes or fast and strong reorganization processes.

This suggests a deep analogy between the dynamics of granular counterflows in the presence of bottlenecks or restrictions and financial price formation processes. The former applies to pedestrians in confined geometries in the presence of constrictions and constraints. The present work extends these ideas to suggest the possible existence of what could be referred to as a new "universality class" for out-of-equilibrium complex extended dynamical systems characterized by "balanced flows with bottlenecks" endowed with the characteristics outlined above and which are described by the set of properties (1)–(8).

Future work will be done to falsify further this suggestion. In particular, the saturated-nonsaturated transition, considering T as the control parameter, could be studied and compared with the fact that financial markets operate close to a critical point in a precise sense [5,41,42]. Also, different regimes of herding behavior within the proposed analogy will be investigated. As the density of particles is varied from dilute gas to liquid and glass, the effect of the bottleneck can be studied systematically with respect to its impact on the density fluctuations in its neighborhood. Similarly to the physics of lubrication and/or of wetting, novel critical behavior and transitions can be expected to translate into an interesting classification of fluctuations in systems characterized by balanced flows with bottlenecks.

The similarity between the granular counterflows and financial prices can be exploited for the understanding and characterization of certain abnormal market regimes, in analogy with the corresponding pedestrian systems. For instance, when the bottleneck is narrower (opening $L < 4$ m), permanent blockage occur due to the soft attraction, which nucleate clusters around and within the constriction. In finance, this corresponds to the no-trade situation occurring when the liquidity vanishes. It would be interesting to study the properties of the density fluctuation close to this jamming transition in parallel to the corresponding situation in financial markets. Moreover, the size of the price window (the equivalent of the door size) could be measured in financial systems by considering various markets with different depths and their effects on the price dynamics could be characterized.

V. CONCLUSIONS

In this work, we have shown that a pedestrian counterflow system with a bottleneck exhibits several stylized facts that are characteristic for financial systems, if the pedestrian density observed in the conflict zone (around the door) is compared to the logarithm of the price of financial assets.

We find that having two groups of agents with opposite interests (counterflow) is an important precondition to reproduce the stylized facts. When these two groups have a constant number of agents during the simulations (automata agents), we find the following stylized facts: heavy tails of the distribution of returns, aggregational Gaussianity, fast-decaying autocorrelation of return, scaling of the peaks of the distribution of returns, multifractality, and self-similarity. Having agents with adaptive behavior (i.e., changing their state by making decisions) is relevant to explain the slowness of decay of the autocorrelation of absolute returns and the existence of bubbles and crashes. This is due to the occurrence of herding behavior, when agents can change their state, making their decisions depending on the state of the neighbors.

The tendency of agents to mimic other agents is controlled by the parameter T. Depending on its value, the system can be in three regimes: (a) a saturated regime ($T \lesssim 0.07$), where all the agents are in the same state; (b) a nonsaturated regime ($T \gtrsim 0.09$), where the population of both classes of agents are in equilibrium (which is similar to the behavior of automata agents with a fix number of agents in each class); and (c) a transition regime ($0.07 \lesssim T \lesssim 0.09$), in which

the saturated and the nonsaturated regimes alternate during intermittent time periods. In the transition regime, the decay of the autocorrelation of absolute return is much slower than the decay of the autocorrelation of the return, matching very well this interesting stylized fact observed in financial time series.

The properties reported here, obtained for a system with 60 particles, do not change appreciably with varying this number within factors of 2. However, we should stress that the characteristics of the density fluctuations that are so similar to financial price fluctuations depend on the system not being too large. In other words, the stylized facts disappear in the thermodynamic limit and are, thus, intrinsically "finite-size effects." This should not be taken necessarily as a drawback, since there is evidence that the price dynamics of any given financial asset is typically driven by no more than about 100 investors (see, for example, Ref. [22]). We refer to Refs. [43,44] for reviews of the finite-size effects in various models of financial price dynamics.

Nishinari *et al.* [45] have established a connection between traffic jams and bubble bursts by viewing the latter as a jam in transaction volume. This correspondence is based both on empirical data and a one-dimensional model of cash-in-advance cash-house transaction flows. One can relate their work to ours by noting that volume is strongly correlated with volatility, which is a measure of the amplitude of log-price variations.

In conclusion, the statistical analogies between the pedestrian counterflow problem and financial time series suggest that studying pedestrian counterflow systems in the presence of constraints may help to gain a better understanding of the mechanisms underlying stylized facts of financial markets.

ACKNOWLEDGMENTS

D.R.P. is grateful for partial financial support by ETH Zürich and by CONICET (via the Project P.I.P.-0304).

[1] S. Ghashghaie, W. Breymann, J. Peinke, P. Talkner, and Y. Dodge, Nature **381**, 767 (1996).
[2] U. Frisch, *Turbulence: The Legacy of A. N. Kolmogorov* (Cambridge University Press, Cambridge, UK, 1995).
[3] A. Arneodo, J.-P. Bouchaud, R. Cont, J.-F. Muzy, M. Potters, and D. Sornette, Comment on "Turbulent Cascades in Foreign Exchange Markets" [reply to S. Ghashghaie, W. Breymann, J. Peinke, P. Talkner, and Y. Dodge, Nature **381**, 767 (1996)], http://xxx.lanl.gov/abs/cond-mat/9607120.
[4] C. Vamoş, N. Suciu, and W. Blaj, Physica A **287**, 461 (2000).
[5] J.-P. Bouchaud, J. Kockelkoren, and M. Potters, Quant. Financ. **6**, 115 (2006).
[6] P. Bak, M. Paczuski, and M. Shubik, Physica A **246**, 430 (1997).
[7] A. Svorencík and F. Slanina, Eur. Phys. J. B **57**, 453 (2007).
[8] D. Helbing, Phys. Bl. **57**, 27 (2001).
[9] D. Helbing, Rev. Mod. Phys. **73**, 1067 (2001).
[10] D. R. Parisi, Adv. Appl. Stat. Sci. **2**, 347 (2010).
[11] D. Helbing, A. Johansson, and H. Z. Al-Abideen, Phys. Rev. E **75**, 046109 (2007).
[12] M. Moussaïd, D. Helbing, and G. Theraulaz, Proc. Nat. Acad. Sci. USA **108**, 6884 (2008).
[13] D. M. Guillaume, M. M. Dacorogna, R. R. Davé, U. A. Müller, R. B. Olsen, and O. V. Pictet, Financ. Stoch. **1**, 95 (1997).
[14] R. Cont, Quant. Financ. **1**, 223 (2001).
[15] J.-P. Bouchaud and M. Potters, Physica A **299**, 60 (2001).
[16] T. Lux, *Handbook of Financial Markets: Dynamics and Evolution* (Elsevier, Amsterdam, 2009), Chap. 3, pp. 161–215.
[17] Y. Malevergne, and D. Sornette, *Extreme Financial Risks (From Dependence to Risk Management)* (Springer, Heidelberg, 2006).
[18] A. Chakraborti, I. Muni Toke, M. Patriarca, and F. Abergel, Quant. Financ. **11**, 991 (2011).
[19] http://finance.yahoo.com/.
[20] https://www.dukascopy.net/swiss/english/data_feed/csv_data_export/?hl=en.
[21] D. Helbing, I. Farkas, and T. Vicsek, Nature **407**, 487 (2000).
[22] F. Lillo, E. Moro, G. Vaglica, and R. N. Mantegna, New J. Phys. **10**, 043019 (2008).
[23] T. G. Andersen, T. Bollerslev, F. X. Diebold, and P. Labys, Multinational Finance Journal **4**, 159 (2000).
[24] M. A. Virasoro, http://arxiv.org/abs/1112.0770.
[25] Y. Malevergne, V. F. Pisarenko, and D. Sornette, Quant. Financ. **5**, 379 (2005).
[26] J.-P. Bouchaud, and M. Potters, *Theory of Financial Risk and Derivative Pricing: From Statistical Physics to Risk Management*, 2nd ed. (Cambridge University Press, Cambridge, UK, 2009).
[27] B. B. Mandelbrot, J. Bus. **36**, 392 (1963).
[28] L. E. Calvet and A. J. Fisher, *Multifractal Volatility: Theory, Forecasting, and Pricing* (Academic Press, San Diego, CA, 2008).
[29] R. Cont, *Long Memory in Economics* (Springer, Berlin, 2007), pp. 289–309.
[30] R. N. Mantegna and H. E. Stanley, Nature **376**, 46 (1995).
[31] Z. I. Botev, J. F. Grotowski, and D. P. Kroese, Ann. Stat. **38**, 2916 (2010).
[32] B. B. Mandelbrot, *Fractals and Scaling in Finance: Discontinuity, Concentration, Risk*, 1st ed. (Springer, Berlin, 1997).
[33] G. La Spada, J. D. Farmer, and F. Lillo, Eur. Phys. J. B **64**, 607 (2008).
[34] T. Lux and M. Marchesi, Nature **397**, 498 (1999).
[35] C. K. Peng, S. Havlin, H. E. Stanley, and A. L. Goldberger, Chaos **5**, 82 (1995).
[36] G. Harras, C. J. Tessone, and D. Sornette, Phys. Rev. E **85**, 011150 (2012).
[37] A. S. Kyle, Econometrica **53**, 1315 (1985).
[38] G. Huberman and W. Stanzl, Econometrica **72**, 1247 (2004).
[39] Z. Eisler, J.-P. Bouchaud, and J. Kockelkoren, Quant. Financ. **1**, 25 (2011).
[40] J. D. Farmer, A. Gerig, F. Lillo, and H. Waelbroeck, arXiv:1102.5457.
[41] B. Tóth, Y. Lempérière, C. Deremble, J. de Lataillade, J. Kockelkoren, and J.-P. Bouchaud, Phys. Rev. X **1**, 021006 (2011).

[42] V. Filimonov and D. Sornette, Phys. Rev. E **85**, 056108 (2012).
[43] A. Corcos, J.-P. Eckmann, A. Malaspinas, Y. Malevergne, and D. Sornette, Quant. Financ. **2**, 264 (2002).
[44] D. Sornette, D. Stauffer, and H. Takayasu, in *Theories of Disaster: Scaling Laws Governing Weather, Body, and Stock Market Dynamics*, edited by A. Bunde, J. Kropp, and H.-J. Schellnhuber, (Springer-Verlag, Berlin, 2002), http://xxx.lanl.gov/abs/cond-mat/9909439.
[45] K. Nishinari, M. Iwamura, Y. Umeno Saito, and T. Watanabe, J. Phys.: Conf. Ser. **221**, 012006 (2010).